

## Advantages of NiO<sub>x</sub> electrode over Au in low-voltage tetracene-based phototransistors

Jeong-M. Choi, Kimoon Lee, D. K. Hwang, Jae Hoon Kim, and Seongil Im<sup>a)</sup>  
*Institute of Physics and Applied Physics, Yonsei University, Seoul 120-749, Korea*

Ji Hoon Park and Eugene Kim  
*Department of Information Display Engineering, Hongik University, Seoul 121-791, Korea*

(Received 20 September 2006; accepted 21 September 2006; published online 4 December 2006)

We report on the tetracene-based photo-thin-film transistors (photo-TFTs) which adopt thin poly-4-vinylphenol (PVP)/aluminum oxide (AlO<sub>x</sub>) bilayer for a gate dielectric and two different source/drain (*S/D*) electrodes: semitransparent NiO<sub>x</sub> and Au. Our tetracene-based TFT with NiO<sub>x</sub> *S/D* electrode exhibited quite good field effect mobility ( $\mu = \sim 0.23$  cm<sup>2</sup>/V s), high on/off current ratio ( $I_{\text{on}}/I_{\text{off}}$ ) of  $\sim 10^5$ , and good photo-to-dark current ratio ( $I_{\text{ph}}/I_{\text{dark}} = \sim 10^4$ ) under an ultraviolet (364 nm) illumination while that with Au *S/D* electrodes showed much lower device performance ( $\mu = \sim 0.08$  cm<sup>2</sup>/V s,  $I_{\text{on}}/I_{\text{off}} = \sim 10^4$ , and  $I_{\text{ph}}/I_{\text{dark}} = \sim 20$ ), although the both TFTs operated at a low voltage of  $-8$  V. With the hole-injection and light-reception advantages of NiO<sub>x</sub> electrode, our tetracene photo-TFT demonstrated good dynamic optical gating. © 2006 American Institute of Physics. [DOI: 10.1063/1.2396712]

Organic thin-film transistors (OTFTs) have been extensively studied due to their potentials toward driving circuit for display or low-cost logic applications.<sup>1-4</sup> Among many types of OTFTs pentacene-based transistors have been known to be the most promising in terms of field mobility. Tetracene-based TFT does not have a high field mobility compared to pentacene-based TFTs. Therefore they have not been the focus of the present organic electronics research that prefers fast charge transport or fast switching, and thus only a few studies on tetracene TFTs have been reported.<sup>5-8</sup> However, tetracene-based devices could be still in high demand within the framework of optoelectronic and photodetecting area.<sup>6-10</sup> In particular, since pentacene-based devices cannot carry out any photo- or optoelectronic missions despite their excellent dark electronic properties,<sup>10</sup> studies on achieving a high-quality tetracene photo-TFT with an enhanced field mobility and improved photoelectric effects should be again very important for advanced photodevice applications.

In the present study we have fabricated low-voltage tetracene photo-TFTs with thin poly-4-vinylphenol (PVP)/aluminum oxide (AlO<sub>x</sub>) bilayer dielectric, where semitransparent conductive NiO<sub>x</sub> instead of Au has been used for source/drain (*S/D*) electrodes to achieve an enhanced field mobility.

AlO<sub>x</sub> films were deposited on the indium tin oxide (ITO) glass by rf magnetron sputtering using a 2 in. diameter aluminum oxide target (99.999%) in a vacuum chamber at room temperature (RT). The thickness and sheet resistance of the ITO films were 79 nm and 30 Ω/□, respectively. PVP film on AlO<sub>x</sub> layer was then prepared from solutions of PVP and poly(melamine-co-formaldehyde), as a cross-linking agent in propylene glycol monomethyl ether acetate (PGMEA), by

spin coating and subsequent cross-linking (curing) at 175 °C for 1 h in a vacuum oven. The thicknesses of our AlO<sub>x</sub> layer and PVP film were approximately 100 and 45 nm, respectively, as measured by a surface profiler (Alpha-Step IQ). Then, tetracene channels and *S/D* electrodes (NiO<sub>x</sub> or Au) were sequentially patterned on the AlO<sub>x</sub> layer with shadow masks by thermal evaporation. The deposition rate was fixed to 0.1 nm/s for the evaporation of tetracene (Aldrich Chem. Co., ~98% purity) and was controlled to be 3 nm/s for the evaporation of NiO (99.97% purity) and Au. The thicknesses of tetracene, NiO<sub>x</sub>, and Au films were 50, 100, and 200 nm, respectively. The sheet resistance of NiO<sub>x</sub> films was 60–100 Ω/□. Fabricated form of our TFT has a nominal channel length *L* of 90 μm and channel width *W* of 500 μm.

All electrical and photoelectric characterizations were carried out with a semiconductor parameter analyzer (model HP 4155C, Agilent Technologies). Ultraviolet (UV) illumination of 364 nm was performed on our TFTs with a light source (Oriel Optical System). The optical power of the incident monochromatic light was fixed to  $\sim 0.64$  mW/cm<sup>2</sup>. All measurements were performed at RT. Finally, dynamic UV response was measured by a setup composed of our tetracene TFT and a load resistance of 22 MΩ.

Figure 1(a) presents a photograph that displays the plan view of our tetracene-based photo-TFT with semitransparent NiO<sub>x</sub> *S/D* electrode array placed over a paper with small words “tetracene.” Although regions covered with the *S/D* electrode appear darker due to a low transmittance of NiO<sub>x</sub> ( $\sim 30\%$  in the both visible and weak UV ranges)<sup>11</sup> than the tetracene channel or PVP/AlO<sub>x</sub> background area, we can still identify the letters on the paper. Figure 1(b) shows the x-ray diffraction (XRD) (source Cu *K*α) results of our tetracene film grown on PVP/AlO<sub>x</sub>/ITO glass substrates. The organic film deposited on the PVP/AlO<sub>x</sub> bilayer displays good crystallinity and thus these XRD results evidence that the organic crystals grow well on the cross-linked PVP

<sup>a)</sup>Author to whom correspondence should be addressed; electronic mail: semicon@yonsei.ac.kr

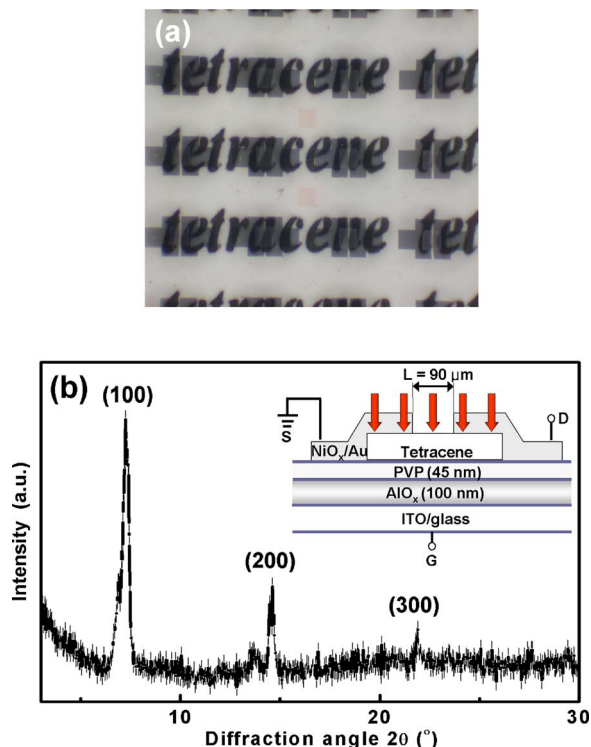


FIG. 1. (Color online) (a) Photographic plan view of our semitransparent TFT array fabricated on glass. (b) XRD pattern of tetracene film deposited on PVP/ $\text{AlO}_x$ /ITO glass substrates. The inset shows the schematic cross section of our tetracene-based TFT with the hybrid bilayer dielectric and semitransparent  $\text{NiO}_x$  S/D area (see the light penetrate the  $\text{NiO}_x$  S/D area in the scheme).

surface.<sup>12,13</sup> The inset of Fig. 1(b) shows the cross section of device structure where our active tetracene layer lies on the PVP/ $\text{AlO}_x$  bilayer dielectric.

The drain current–drain voltage ( $I_D$ - $V_D$ ) characteristics of tetracene-based TFTs with  $\text{NiO}_x$  and Au for S/D electrodes are shown in Figs. 2(a) and 2(b), respectively. Under a gate bias ( $V_G$ ) of  $-8$  V our TFT with  $\text{NiO}_x$  S/D electrode has a much higher saturation current of  $0.37 \mu\text{A}$  than that with Au S/D, which shows only about  $\sim 0.06 \mu\text{A}$ . These low-voltage operations were basically possible due to the bilayer dielectric approach that enables good organic crystal growth

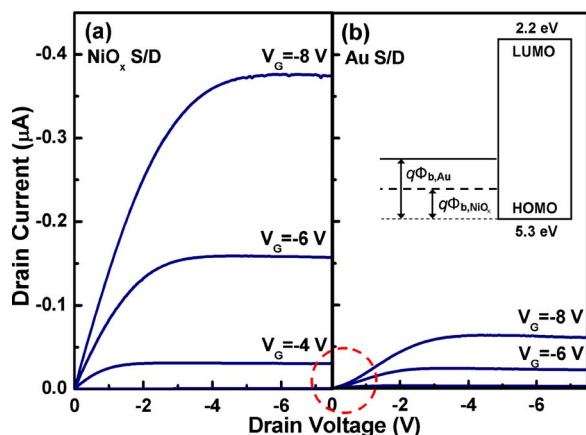


FIG. 2. (Color online)  $I_D$  vs  $V_D$  characteristics of our OTFT with (a)  $\text{NiO}_x$  and (b) Au S/D electrodes. The inset shows a simplified energy band diagram of tetracene interfaced with  $\text{NiO}_x$  and with Au.

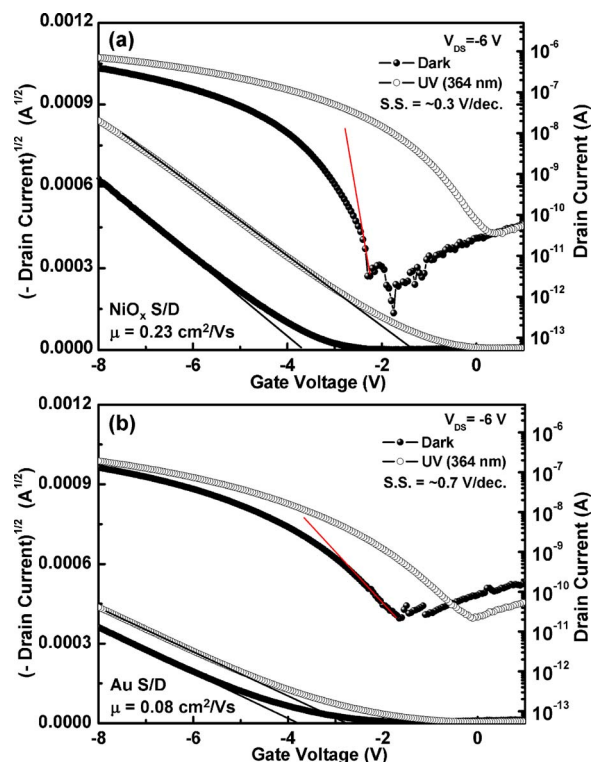


FIG. 3. (Color online)  $\sqrt{-I_D}$  vs  $V_G$  and  $\log(-I_D)$  vs  $V_G$  curves obtained from our tetracene-based photo-TFT with (a)  $\text{NiO}_x$  and (b) Au S/D electrodes at  $V_{D_S} = -6$  V. Our tetracene-based TFTs were illuminated by UV (364 nm,  $0.64 \text{ mW}/\text{cm}^2$ ) lights.

and considerable dielectric charging on the PVP surface. Here, our PVP (45 nm)/ $\text{AlO}_x$  (100 nm) hybrid bilayer dielectric appeared to have  $31 \text{ nF}/\text{cm}^2$  and  $4 \text{ MV}/\text{cm}$  for its dielectric capacitance and strength, respectively. More details about the bilayer dielectric approaches would be found elsewhere.<sup>12,13</sup> Our main purpose in the present work, however, is to enhance the field mobility of tetracene TFT with those dielectrics by using  $\text{NiO}_x$  electrode, so that our tetracene photo-TFT may well transport photogenerated carriers. The work function level of the thermally evaporated  $\text{NiO}_x$  is known to be larger<sup>14</sup> than that of Au and thus should be better matched with the highest occupied molecular orbital (HOMO) ( $\sim 5.3 \text{ eV}$ ) of tetracene.<sup>15</sup> According to a simplified energy band diagram of tetracene relative to the work function levels of  $\text{NiO}_x$  and Au [the inset of Fig. 2(b)], the injection of holes by  $\text{NiO}_x$  to the HOMO of tetracene should be much easier than from Au because the injection barrier of the former case is smaller than that of the latter. Based on our recent work function studies on the thermally evaporated  $\text{NiO}_x$  and Au, the barriers for Au/tetracene ( $q\Phi_{b,\text{Au}}$ ) and  $\text{NiO}_x$ /tetracene ( $q\Phi_{b,\text{NiO}_x}$ ) are estimated to be  $0.55$  and  $0.2 \text{ eV}$ , respectively.<sup>14</sup> As for the OTFT using Au S/D on tetracene, non-Ohmic behavior is also noted, in particular, from the initial  $V_D$  stages [see the dotted circle in Fig. 2(b)], giving further evidence for its large injection barrier height or higher contact resistance.

The  $I_D$ - $V_G$  relationships were obtained from our tetracene-based TFTs with  $\text{NiO}_x$  [Fig. 3(a)] and Au [Fig. 3(b)] electrodes at  $V_D = -6$  V. According to the  $\log(-I_D)$  vs  $V_G$  and the  $\sqrt{-I_D}$  vs  $V_G$  curves, our tetracene OTFT with the

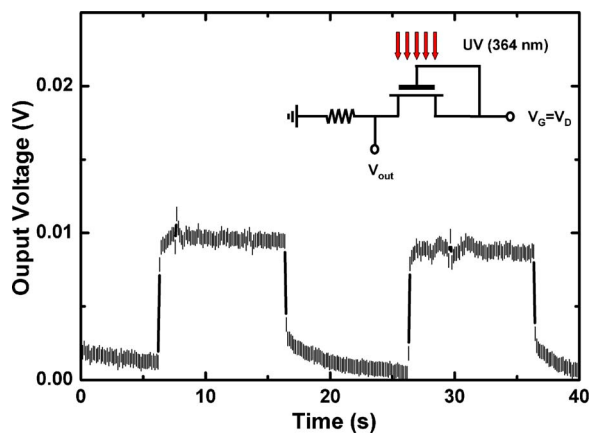


FIG. 4. (Color online) Dynamic photoinduced output signals obtained from a measurement setup (inset) involving our tetracene-based TFT with NiO<sub>x</sub> and a 22 MΩ resistor. UV modulated with 0.1 Hz turns on and off our TFT.

NiO<sub>x</sub> electrode showed a high mobility of 0.23 cm<sup>2</sup>/V s (saturation regime mobility), a high on/off current ratio of  $\sim 10^5$ , and an excellent subthreshold slope (SS) of 0.3 V/decade, while the performances of a similar OTFT with Au were limited to a lower mobility of 0.08 cm<sup>2</sup>/V s with a lower on/off ratio of  $\sim 10^4$  and an inferior SS of 0.7 V/decade. Since the reported mobility of single crystalline tetracene is  $\sim 0.4$  cm<sup>2</sup>/V s (Ref. 16), our presented mobility (0.23 cm<sup>2</sup>/V s) is quite a high and enhanced value as obtained by improving the contact resistance and the dielectric layer design. Threshold voltage ( $V_T$ ) of the both TFTs with NiO<sub>x</sub> and Au was about the same as  $-3.7$  V.

Our tetracene TFT with NiO<sub>x</sub> also responded more sensitively to light than that with Au. The tetracene TFT with NiO<sub>x</sub> was turned on by UV light at a low gate voltage of  $-1.2$  V and showed a high photo-to-dark current ratio ( $I_{ph}/I_{dark}$ ) of  $\sim 10^4$  [Fig. 3(a)], while that with Au showed a high turn-on voltage of  $-2.8$  V under UV light with a low  $I_{ph}/I_{dark}$  of only  $\sim 20$  [Fig. 3(b)] ( $I_{dark}$  was taken to be the minimum current at  $V_G = -2$  V). Such improved photoelectric performance is because the semitransparent NiO<sub>x</sub> *S/D* electrode could also be used as a photon window. Since our NiO<sub>x</sub> has an optical energy gap of  $\sim 4.1$  eV and 30% transmittance for weak UV lights,<sup>11</sup> considerable amount of incident 364 nm UV photons could penetrate our *S/D* window area to excite the depleted tetracene below NiO<sub>x</sub> as well as to excite the open channel area not covered by the *S/D* electrode [see the inset device scheme of Fig. 1(b)]. Therefore, our tetracene TFT with NiO<sub>x</sub> *S/D* is probably an advanced model for organic photo-TFTs, along with its enhanced dark electric properties as presented above.

Dynamic UV response of our tetracene TFTs was also tested through a measurement setup that includes the tetracene TFT and a load resistance of 22 MΩ. Figure 4 shows the output voltage signals obtained from the setup. When a low constant bias of  $-3$  V was applied to the gate and drain of our TFT, the tetracene TFT might be in off state (depletion state,  $V_T = \sim -3.5$  V) in the dark. The tetracene-based TFT

was periodically turned on by a 364 nm UV light (with a low modulation frequency of 0.1 Hz and an optical power density of 0.64 mW/cm<sup>2</sup>). The output (voltage) signal due to the photoinduced current was observed in the time domain. Since the initial UV response time was as short as  $\sim 300$  ms but a few seconds of lagging (probably due to the intrinsic deep level defects in tetracene) was also observed in falling (turn off), the dynamic performance of our tetracene TFT is probably not comparable to those of inorganic devices. However, such dynamic response or optical gating behavior from any organic TFTs has rarely been reported.

In summary, we have fabricated low-voltage tetracene-based photo-TFTs with thin PVP/AlO<sub>x</sub> bilayer dielectric. When two electrodes of Au and semitransparent NiO<sub>x</sub> are adopted for *S/D*, the tetracene-based TFTs with NiO<sub>x</sub> exhibited higher field mobility than those with Au due to the band alignment advantage of NiO<sub>x</sub> over Au. Our tetracene TFT with NiO<sub>x</sub> also showed much higher static photoresponse ( $I_{ph}/I_{dark}$  of  $\sim 10^4$ ) than that with Au because of the NiO<sub>x</sub> photon window. Based on the good photoresponse, UV-induced dynamic gating was demonstrated under a gate bias of  $-3$  V. It is concluded that our tetracene-based TFT jointly adopting NiO<sub>x</sub> for the *S/D* electrode and PVP/AlO<sub>x</sub> bilayer for gate dielectric can be an advanced form of photodetecting organic device operating at low voltages.

This research was performed with the financial support from KOSEF (Program No. M1-0214-00-0228) and LG.Philips LCD (project year 2005). They also acknowledge the support from Brain Korea 21 Project and Seoul Science Fellowship.

- <sup>1</sup>C. D. Dimitrakopoulos and P. R. L. Malenfant, *Adv. Mater.* (Weinheim, Ger.) **14**, 99 (2002).
- <sup>2</sup>F. Eder, H. Klauk, M. Halik, U. Zschieschang, G. Schmid, and C. Dehm, *Appl. Phys. Lett.* **84**, 2673 (2004).
- <sup>3</sup>L.-L. Chua, R. H. Friend, and P. K. H. Ho, *Appl. Phys. Lett.* **87**, 253512 (2005).
- <sup>4</sup>H. E. A. Huitema *et al.*, *Nature* (London) **414**, 599 (2001).
- <sup>5</sup>D. J. Gundlach, J. A. Nichols, L. Zhou, and T. N. Jackson, *Appl. Phys. Lett.* **80**, 2925 (2002).
- <sup>6</sup>A. Hepp, H. Heil, W. Weise, M. Ahles, R. Schmechel, and H. V. Seggern, *Phys. Rev. Lett.* **91**, 157406 (2003).
- <sup>7</sup>C. Santato, I. Manunza, A. Bonfiglio, F. Cicoira, P. Cosseddu, R. Zamboni, and M. Muccini, *Appl. Phys. Lett.* **86**, 141106 (2005).
- <sup>8</sup>J. Reynaert, D. Cheyns, D. Janssen, R. Müller, V. I. Arkhipov, J. Genoe, G. Borghs, and P. Heremans, *J. Appl. Phys.* **97**, 114501 (2005).
- <sup>9</sup>E.-A. You, Y.-G. Ha, Y.-S. Choi, and J.-H. Choi, *Synth. Met.* **153**, 209 (2005).
- <sup>10</sup>J.-M. Choi, J. Lee, D. K. Hwang, J. H. Kim, S. Im, and E. Kim, *Appl. Phys. Lett.* **88**, 043508 (2006).
- <sup>11</sup>J.-M. Choi, D. K. Hwang, J. H. Kim, and S. Im, *Appl. Phys. Lett.* **86**, 123505 (2005).
- <sup>12</sup>J.-M. Choi, K. Lee, D. K. Hwang, J. H. Park, E. Kim, and S. Im, *Electrochem. Solid-State Lett.* **9**, G289 (2006).
- <sup>13</sup>D. K. Hwang, K. Lee, J. H. Kim, S. Im, C. S. Kim, H. K. Baik, J. H. Park, and E. Kim, *Appl. Phys. Lett.* **88**, 243513 (2006).
- <sup>14</sup>K. Lee, J. H. Kim, and S. Im, *Appl. Phys. Lett.* **88**, 023504 (2006).
- <sup>15</sup>J. Sworakowski and J. Ulanski, *Annu. Rep. Prog. Chem., Sect. C: Phys. Chem.* **99**, 87 (2003).
- <sup>16</sup>R. W. I. de Boer, T. M. Klapwijk, and A. F. Morpurgo, *Appl. Phys. Lett.* **83**, 4345 (2003).